Determination of the structure of the high-pressure phase of $AuAl_2$ with the help of first-principles calculations

2008 J. Phys.: Condens. Matter 20 325215

(http://iopscience.iop.org/0953-8984/20/32/325215)

IOP PUBLISHING JOURNAL OF PHYSICS: CONDENSED MATTER

J. Phys.: Condens. Matter **20** (2008) 325215 (5pp) doi:10.1088/0953-8984/20/32/325215

Determination of the structure of the high-pressure phase of $AuAl_2$ with the help of first-principles calculations

Ashok K Verma, P Modak and Surinder M Sharma

High Pressure Physics Division, Bhabha Atomic Research Centre, Trombay, Mumbai 400085, India

Received 12 December 2007, in final form 6 June 2008
Published 9 July 2008
Online at stacks.iop.org/JPhysCM/20/325215

Abstract

The high-pressure structural phase transition in $AuAl_2$ is studied using first-principles density functional theory. Our theoretical results predict a structural phase transition at ∼18.7 GPa and the high-pressure phase is identified to be a primitive orthorhombic structure. In addition, our electronic structure calculations rationalize the observed variation of electrical resistance with pressure.

(Some figures in this article are in colour only in the electronic version)

1. Introduction

Pressure-induced structural phase transitions in solids are ubiquitous and the microscopic understanding of phase transformations has led to substantial progress in condensed matter physics. Theoretical and experimental studies of structural phase transitions continue to be one of the very active fields in high-pressure condensed matter physics [1, 2]. The diamond anvil cell (DAC) coupled with intense synchrotron x-ray beams has provided an enormous impetus to these experimental investigations. Though the DAC synchrotron data is quite reliable it is limited in **k** space which may lead to ambiguous structural solutions [3–5]. The structure determination requires hit and miss (with symmetry considerations) or computational work, either based on first-principles density functional methods or sometimes even classical molecular dynamical simulations. But in recent years density functional theory based calculations have provided great insight into the properties of materials near phase transitions as well as into the driving mechanism thereof [6]. Generally, the structural determinations are carried out by calculating the total energy for different possible arrangements of atoms over a wide range of pressures using the density functional theory based methods [7, 8]. Thus one can determine the possible structural phase transition by comparing the pressure variation of enthalpies for different atomic arrangements, i.e. different crystal structures.

In this paper we report results of our first-principles density functional theory calculations for the $AuAl_2$ intermetallic under pressure. Using this, we have predicted the crystal structure of the high-pressure phase. The intermetallics of gold (Au) and platinum (Pt) with aluminum (Al), gallium (Ga) and indium (In) have received considerable attention in the past, due to their fundamental and technological importance [9]. Many of these compounds have been demonstrated to be superconducting at low temperatures [10]. At ambient conditions, these intermetallics have good electrical conductivity and exist in the cubic fluorite structure (CaF_2). In contrast to this, most of the fluorite structure materials are halides, oxides or chalcogenides of univalent or tetravalent cations and show predominantly ionic bonding. These intermetallics also serve as prototypes for studying the variations in the 5d bands at larger A–A separations (A = Au/Pt) compared to those existing in pure A (Au or Pt). Some of these intermetallics are known to show electronic topological transitions (ETT) under pressure [11, 12]. To study ETT in $AuAl_2$, Garg *et al* [3] measured electrical resistance up to 25 GPa pressure and they observed the continuous resistance decrease up to 12 GPa pressure. Above about 12.5 GPa pressure, resistance started increasing slowly and beyond 16 GPa pressure a much faster increase was observed. An explanation for the observed resistance variation with pressure in terms of detailed band structure calculations failed as calculations ruled out the occurrence of ETT. Thus a probable structural phase transition at ∼16 GPa was guessed [3]. Subsequent x-ray diffraction measurements by them confirmed a structural phase transition near 17 GPa. But they were unable to determine the crystal structure of the high-pressure phase due to the presence of only a few diffraction lines relevant to this phase.

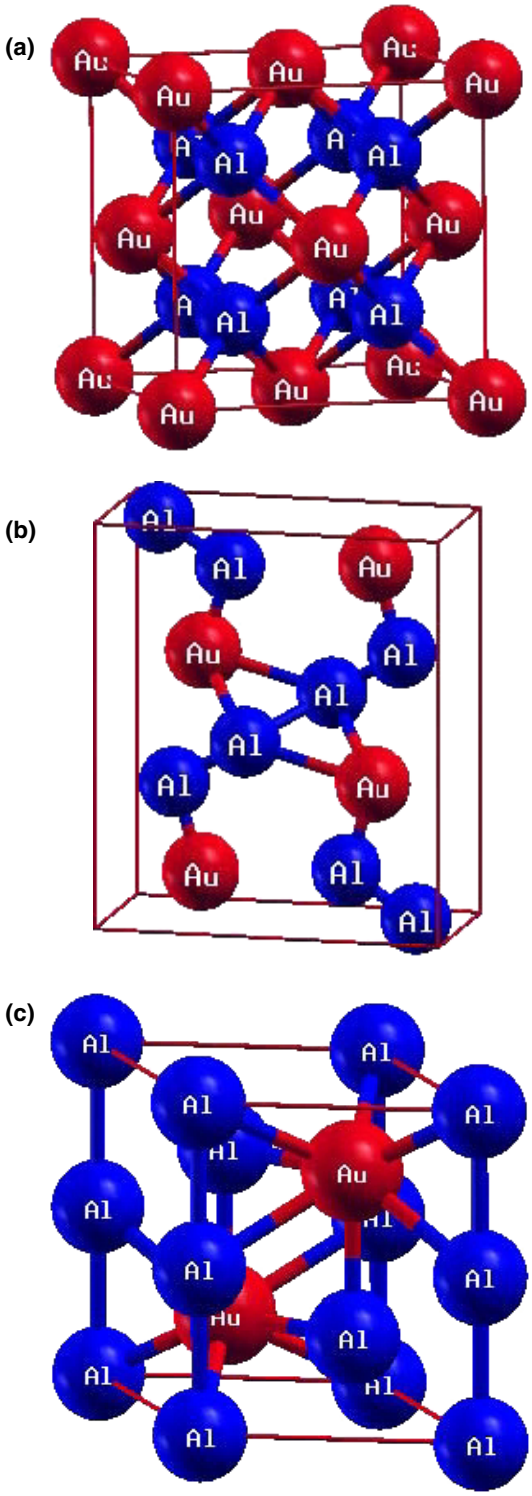

Figure 1. Crystal structures of $AuAl_2$ used in our calculations. (a) Calcium fluorite ($Fm\bar{3}m$), (b) orthorhombic ($Pnma$), and (c) hexagonal ($P6_3/mmc$).

In order to determine a possible crystal structure of the high-pressure phase, we have carried out total energy calculations for three structures, namely, cubic fluorite (SG: $Fm\bar{3}m$), orthorhombic (SG: $Pnma$) and hexagonal (SG: $P6_3/mmc$) as a function of pressure. The reason for choosing only these structures is based on the fact that CaF_2 itself is known to undergo the $Fm\bar{3}m$-to-$Pnma$-to-$P6_3/mmc$ series of transformations under pressure [13, 14]. In our study, we have fully optimized the internal (fractional) atomic coordinates and cell parameters of the orthorhombic and hexagonal structures at several densities. We find that, at pressures close to the experimental value, $AuAl_2$ transforms to an orthorhombic structure ($Pnma$), very similar to the CaF_2. Our calculations also help in rationalizing the observed pressure variation of resistance in terms of the change in the density of states across the cubic CaF_2-to-orthorhombic $Pnma$ structural transition.

Table 1. Comparison of the calculated quantities with the experimental.

Properties	Theory	Experimental [3]
a (Å)	6.066	6.005
B (GPa)	104	111
B'	4.83	4.00

2. Method of calculations

All the calculations were performed using the Vienna *ab initio* simulation package (VASP) which is based on the pseudopotential density functional technique. We have used projector augmented wave (PAW) pseudopotentials which were generated using the valence configuration s^1d^{10} for Au and s^2p^1 for Al [15–17]. For the exchange–correlations terms the generalized-gradient approximation of Perdew–Burke–Ernzerhof (GGA-PBE) was used [18]. To chose the plane wave basis set an energy cutoff of 500 eV is taken in our calculations. The Brillouin zone (BZ) samplings were carried out using 275 **k** points in the irreducible wedge of the BZ for the cubic structure, 200 **k** points for the orthorhombic structure and 231 **k** points for the hexagonal structure. The Monkhorst–Pack method was employed for the **k**-point generation in the BZ [19]. The forces on atoms were converged to 10^{-4} eV $Å^{-1}$. The energy convergence with respect to **k** points in the BZ sampling and plane wave energy cutoff has been carefully evaluated. All the atomic coordinates and cell parameters of the high-pressure phases were optimized at several densities. All three crystal structures are shown in figure 1. These structures were generated using the *Xcrysden* computer software [20].

3. Results and discussion

For the ambient structure (i.e. cubic CaF_2), several observables such as equilibrium volume (thus lattice constant), bulk modulus (B) and its first pressure derivative (B') were estimated from the calculated total energy as a function of volume. All these quantities are given in table 1 along with available experimental data. To obtain the equilibrium volume, the energy–volume data was fitted to a fourth-order polynomial and the equilibrium volume was identified from the minimum of the curve. The computed equilibrium volume is overestimated by ∼3% compared to the experimental value, a very common feature of GGA exchange–correlations as it

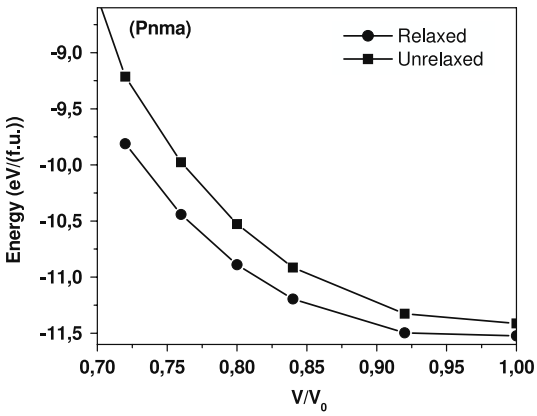

Figure 2. The variation in the total energy on relaxation, as a function of compression for the orthorhombic structure of $AuAl_2$.

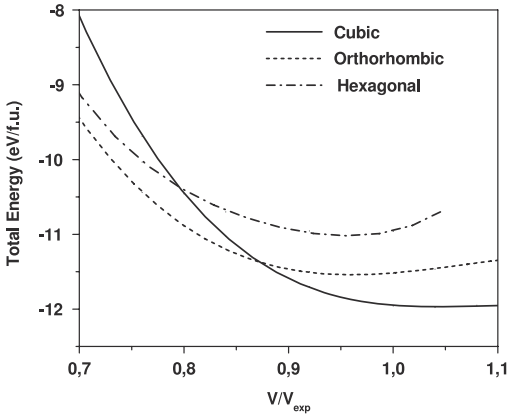

Figure 3. Computed variations in the total energies with volume compression for all three different structures of $AuAl_2$.

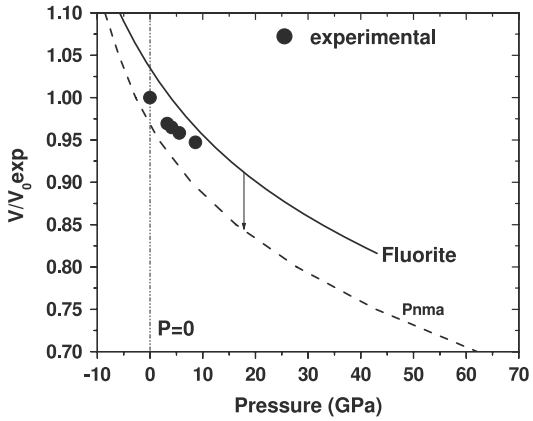

Figure 4. Pressure–volume equation of states for $AuAl_2$. Here the arrow indicates the transition pressure and the experimental data is from [3]. The V_0 exp is the cubic phase equilibrium volume from [3].

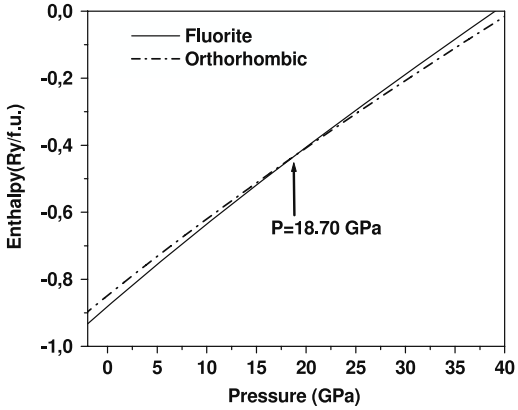

Figure 5. Enthalpy variation of $AuAl_2$ with pressure in $Fm\bar{3}m$ and $Pnma$ (relaxed) structures.

underbinds the solids. This value is within the typical and acceptable range of the density functional based first-principles calculations. The computed bulk modulus, 104 GPa, is also underestimated due to the under-binding given by GGA. The calculated value of the pressure derivative of the bulk modulus is 4.85, which matches reasonably with the experimental value of 4.0 [3]. Using these values of bulk modulus and equilibrium volumes, our estimated Debye temperature (289 K) is in good agreement with the experimental value of 297 K [21, 22].

For the high-pressure phase of the $AuAl_2$ intermetallic the post fluorite structure, i.e. orthorhombic ($Pnma$), was the first choice [13]. Starting from this structure, we determined the equilibrium parameters by relaxing with respect to cell parameters and the fractional atomic coordinates. The total energy of relaxed and unrelaxed structures with volume compression for the orthorhombic ($Pnma$) is shown in figure 2. Here unrelaxed means the structural parameters (i.e. b/a, c/a ratios and internal atomic coordinates) are as for the CaF_2 structure [14]. One can notice that at $V/V_0 = 1.0$ the energy change on relaxation is by 127 meV per formula unit (f.u.) and this change in energy increases with volume compression. For $V/V_0 = 0.718$ the energy change is about 614 meV/f.u. These observations point out the necessity of the structural relaxation for the computations which deal with the studies related to the phase transitions.

Total energy for the relaxed orthorhombic and hexagonal structures is compared with that of the ambient cubic fluorite structure and results are depicted in figure 3. From this it is evident that, beyond ∼13% compression, the orthorhombic $Pnma$ structure becomes lower in energy compared to the other two structures, thus implying a structural phase transition from cubic fluorite to orthorhombic $Pnma$ structure at this compression. Using our energy versus volume results, we calculated the pressure–volume equation of state for $Fm\bar{3}m$ and $Pnma$ structures and these are shown in figure 4 along with experimentally available data points. To determine the structural transition pressure, we estimated the structural enthalpies for the ambient ($Fm\bar{3}m$) and the high-pressure ($Pnma$) phases as a function of pressure. The results are displayed in figure 5. Our calculated transition pressure is 18.7 GPa, which is in very good agreement with the experimental value of transition pressure (∼17 GPa) [3], thus supporting the possibility that the new structure may be $Pnma$. The optimized structural parameters just above the transition pressure for the orthorhombic structure are given

Table 2. Structural parameters of high-pressure phase. The parameters in square brackets are from [3]. Here we took the longest cell edge (denoted by c) along the z axis and the smallest cell edge (denoted by b) along the y-axis. The difference in a between theory and experiment is largely due to cell volume differences.

Theory	Rietveld refined
Au (4c): (0.2532, 0.25, 0.1300)	Au (4c): (0.2767, 0.25, 0.1317)
Al1 (4c): (0.3837, 0.25, 0.4163)	Al1 (4c): (0.4039, 0.25, 0.4556)
Al2 (4c): (0.0558, 0.25, 0.3484)	Al2 (4c): (00.2005, 0.25, 0.3473)
$a = 6.9735$ Å, $b/a = 0.469$, $c/a = 1.139$	$a = 7.414$ [7.472], $b/a = 0.476$ [0.425], $c/a = 1.10$ [1.08]

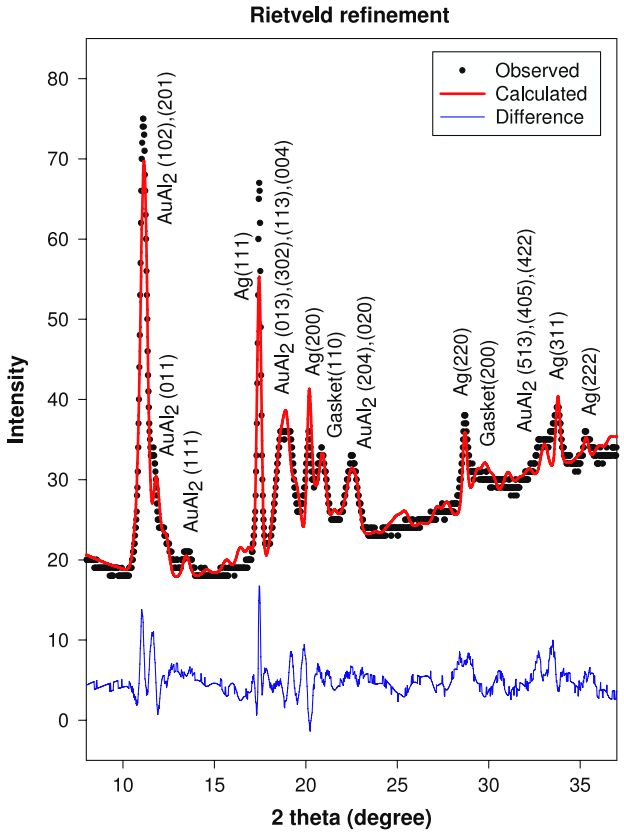

Figure 6. Rietveld refinement with *Pnma* space group.

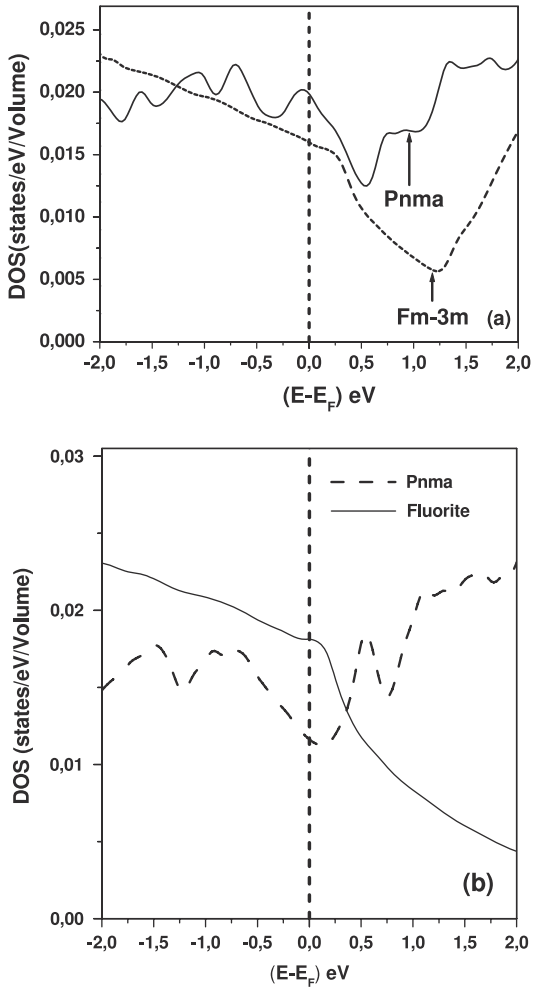

Figure 7. Electronic DOS for different structures (a) at ambient pressure, (b) at 18.7 GPa pressure.

in table 2. The theoretically optimized structure resulted in a good match with the experimental diffraction pattern (see figure 6). Starting from the first-principles relaxed values of atomic coordinates (table 2), we could do the Rietveld analysis and obtain the final fractional coordinates for the orthorhombic phase. Obviously some of the values have drifted away from the initial estimates (i.e. theoretical values), but it leads to excellent agreement with the experimental diffraction pattern (figure 6). Also, we compared our Rietveld refined lattice parameters with that of [3] (see table 2).

To explain the observed high-pressure resistance behavior qualitatively, we make use of the Bloch resistivity formula derived for electrons with a parabolic dispersion scattering from acoustic Debye phonons [23], i.e.

$$\rho = \frac{3\pi\hbar Q^6 n^2}{8e^2\varepsilon_F D(\varepsilon_F)^2 N k_B \theta_D k_F^4}\left(\frac{T}{\theta_D}\right)^5 I_5\left(\frac{\theta_D}{T}\right). \qquad (1)$$

Here n is the electron density, ε_F is the Fermi energy, Q is a phonon wavevector, $D(\varepsilon_F)$ is the density of states (DOS) per unit volume, i.e. specific density of states, θ_D is the Debye temperature, k_F is the Fermi vector and I_5 is a Debye integral given by

$$I_5(x) = \int_0^x \frac{z^5 e^z}{(e^z - 1)^2}\,dz. \qquad (2)$$

Expressing ε_F and k_F in terms of n and $D(\varepsilon_F)$, the Bloch formula can be written as

$$\rho = \frac{\pi^2\hbar Q^6 n^{-1/2}}{4e^2 D(\varepsilon_F) k_B \theta_D}\left(\frac{T}{\theta_D}\right)^5 I_5\left(\frac{\theta_D}{T}\right). \qquad (3)$$

Equation (3) shows that, at a given temperature, the resistivity of a metal correlates inversely with the specific electronic DOS

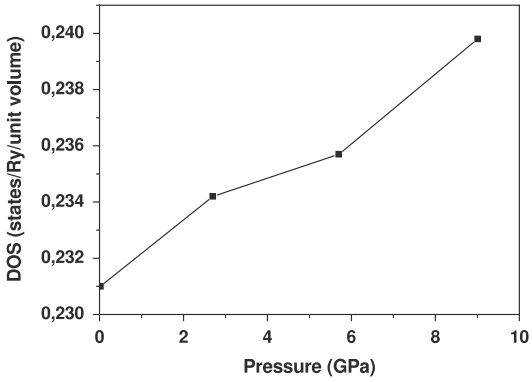

Figure 8. Specific electronic DOS for cubic fluorite phase variation with pressure.

(i.e. DOS/unit volume) at the Fermi level (E_F). The calculated specific DOS at 0 and 18.7 GPa pressure for cubic ($Fm\bar{3}m$) and orthorhombic ($Pnma$) structures with fully relaxed structures is shown in figure 7. One can see that the cubic phase has the lower specific DOS at the Fermi level than the orthorhombic phase. As shown in figure 7(b), we find that, near 18.7 GPa pressure, the specific DOS at E_F for the orthorhombic $Pnma$ structure is smaller by almost 25% compared to that of the cubic phase. This substantial decrease in specific density of states at the Fermi level across the phase transition would imply much larger resistivity in the daughter phase (if the other terms in equation (3) do not change appreciably with the structural transition), in agreement with experimental findings [3]. Thus one would expect an abrupt jump in the resistance across the cubic-to-orthorhombic phase transition. But, being a first-order transition, the daughter phase will grow gradually and thus one would expect that resistance in the mixed phase will increase smoothly until the transition is completed. Our calculations also show that in the cubic phase the specific DOS at E_F increases slowly with pressure, implying a gradual decrease of resistance below 10 GPa pressure region (figure 8).

4. Conclusions

Our *ab initio* total energy calculations, coupled with the structural relaxation calculations, predict the high-pressure phase of $AuAl_2$ to be orthorhombic ($Pnma$). This high-pressure structure is the same as that observed in CaF_2 at high pressure [9]. Our calculated specific electronic DOS at the Fermi level provides qualitative interpretation of the observed pressure-induced change in the resistance.

Acknowledgments

We thank Dr Alka B Garg for providing us with the high-pressure x-ray diffraction data and Mr K K Pandey for the Rietveld refinement.

References

[1] Samara G A 1986 *Physica* **139/140** B3
[2] McMahon M I and Nelmes R J 2006 *Chem. Soc. Rev.* **35** 943
[3] Garg A B, Verma A K, Vijayakumar V, Rao R S and Godwal B K 2005 *Phys. Rev.* B **72** 024112
[4] Gregoryanz E, Sanloup C, Somayazulu M, Badro J, Fiquet G, Mao H-K and Hemley R 2004 *Nat. Mater.* **3** 294
[5] Young A F, Sanloup C, Gregoryanz E, Scandolo S, Hemley R J and Mao H-K 2006 *Phys. Rev. Lett.* **96** 155501
[6] Young A F, Montoya J A, Sanloup C, Lazzeri M, Gregoryanz E and Scandolo S 2006 *Phys. Rev.* B **73** 153102
[7] Hohenberg P C and Kohn W 1964 *Phys. Rev.* B **136** 864
[8] Kohn W and Sham L J 1965 *Phys. Rev.* A **140** 1133
[9] Hahn E and Seraphin B O 1978 *Phys. Thin Film* **10** 1
[10] Wernick J H, Menth A, Geballe T H, Hull G and Maita J P 1969 *J. Phys. Chem. Solids* **30** 1949
[11] Godwal B K, Meenakshi S, Modak P, Rao R S, Sikka S K, Vijayakumar V, Bussetto E and Lausi A 2002 *Phys. Rev.* **B 65** R140101
[12] Garg A B, Godwal B K, Meenakshi S, Modak P, Rao R S, Sikka S K, Vijayakumar V, Lausi A and Bussetto E 2002 *J. Phys.: Condens. Matter* **14** 10605
[13] Seifert K F and Bunsenges Ber 1966 *Phys. Chem.* **70** 1041
[14] Xiang W, Shan Q and Ziyu W 2006 *Phys. Rev.* B **73** 134103
[15] Kresse G and Furthmuller J 1996 *Phys. Rev.* B **54** 11169
[16] Kresse G and Hafner J 1993 *Phys. Rev.* B **47** 558
[17] Kresse G and Joubert J 1999 *Phys. Rev.* B **59** 1758
[18] Perdew J P, Burke K and Ernzerhof M 1996 *Phys. Rev. Lett.* **77** 3865
[19] Monkhorst H J and Pack J D 1976 *Phys. Rev.* B **13** 5188
Monkhorst H J and Pack J D 1977 *Phys. Rev.* B **16** 1748
[20] Kokalj A 2003 *Comput. Mater. Sci.* **28** 155
[21] Asfcroft N W and Mermin N D 1976 *Solid State Physics* (Philadelphia, PA: Saunders College Publishing)
[22] Rayne J A 1963 *Phys. Lett.* **7** 114
[23] Ziman J M 1967 *Electrons and Phonons* (Oxford: Oxford University Press) p 364